NJC

RSC Publishing

PAPER

View Article Online
View Journal | View Issue

Facile one-pot synthesis of lepidocrocite (γ-FeOOH) nanoflakes for water treatment

Cite this: *New J. Chem.*, 2013, **37**, 2551

Yong Jia,[ab] Tao Luo,[a] Xin-Yao Yu,[a] Zhen Jin,[a] Bai Sun,[a] Jin-Huai Liu[a] and Xing-Jiu Huang*[a]

Received (in Montpellier, France) 13th May 2013,
Accepted 4th June 2013

DOI: 10.1039/c3nj00509g

www.rsc.org/njc

Lepidocrocite (γ-FeOOH) nanoflakes were synthesized using a simple ethylene glycol (EG) mediated solution method. The obtained γ-FeOOH were characterized by X-ray diffraction, X-ray photoelectron spectroscopy, field emission scanning electron microscopy, transmission electron microscopy, and nitrogen adsorption–desorption isotherms. The absoption properties of the as-prepared γ-FeOOH nanoflakes towards toxic As(v) and Cr(vi) ions were investigated. The effects of anions such as Cl^-, SO_4^{2-}, NO_3^-, HCO_3^-, CO_3^{2-}, and PO_4^{3-} on As(v) removal were also investigated. The results indicated that phosphate was the greatest competitor with As(v) for adsorptive sites. The presence of Cl^-, SO_4^{2-}, and NO_3^- had no effect on As(v) removal.

Introduction

Recently, the removal of arsenic from drinking water has attracted great attention because of its toxicity.[1] An adsorption method has been proven to be a promising technology for water purification, owing to its high efficiency and ease of operation. For the adsorbent, metal oxides are very important because of their remarkable advantages, such as low cost and easy preparation. So, various metal oxide adsorbents have been synthesized for arsenic removal, for example, CeO_2,[2] CuO,[3] Al_2O_3,[4] Fe_3O_4,[5] and $MgFe_2O_4$,[6] Fe_3O_4–NiO,[7] Fe_3O_4–MnO_2[8] hybrid oxides. In particular, iron oxyhydroxides have attracted great attention owing to their low cost, natural abundance, excellent adsorption and photocatalytic properties for environmental applications.[9–12] Among them is γ-FeOOH, although it appears to be thermodynamically metastable with respect to other ferric oxyhydroxides,[13,14] and it has been proved to be an important functional material in photocatalytic processes.[15–19] Furthermore, γ-FeOOH has exhibited a good adsorption performance towards selenate.[20] Recently, the adsorption properties of γ-FeOOH towards arsenic were investigated,[21] but the preparation process of it was complicated and required some toxic reagents.

Several methods have been reported for the synthesis of γ-FeOOH, such as the oxidation of Fe(ii) ions[13,21–24] or Fe(ii) complexes,[14,17,18,20] electrodeposition of Fe(iii) ions,[25,26] and the controlled hydrolysis of Fe(iii) ions.[27] However, these reported methods are complex and require some special ancillary facilities or oxidizing/reducing agents. In our previous work, we reported the synthesis of some inorganic nanostructures using a simple solution strategy,[28–30] including Fe_3O_4/α-FeOOH microspheres.[10] Herein, based on a similar method, three-dimensional (3D) γ-FeOOH nanoflakes with a high surface area of 132.8 $m^2\ g^{-1}$ were synthesized using a simple ethylene glycol (EG) mediated solution method at 100 °C for the first time. The obtained γ-FeOOH nanoflakes present good removal properties towards toxic As(v) and Cr(vi) ions.

Experimental

Materials and adsorbent preparation

All the chemicals used were of analytical grade and were purchased from Shanghai Chemical Reagents Company and used without further purification. In a typical synthesis process, 4.04 g of $Fe(NO_3)_3{\cdot}9H_2O$ was dissolved in a mixed solution of 50 mL deionized water and 50 mL EG at room temperature. After that, 2.4 g of urea was added to the solution. After stirring for 10 minutes, the solution was transferred into a conical flask with a stopper, and then heated at 100 °C for 12 h and allowed to cool to room temperature naturally. The resulting deep-orange precipitates were collected by centrifugation and washed with deionized water repeatedly until a neutral pH was achieved. The obtained precipitates were then dried at 60 °C.

[a] *Research Center for Biomimetic Functional Materials and Sensing Devices, Institute of Intelligent Machines, Chinese Academy of Sciences, Hefei 230031, PR China. E-mail: xingjiuhuang@iim.ac.cn; Fax: +86 551 65592420; Tel: +86 551 65591142*

[b] *Department of Pharmacy, Anhui University of Chinese Medicine, Hefei 230031, PR China*

Characterization

The as-prepared product was characterized by field emission scanning electron microscopy (FEI Sirion 200 FEG, operated at 10 kV), transmission electron microscopy (JEOL-2010, operated at 200 kV), X-ray diffraction (X'Pert ProMPD, Cu-Kα radiation, wavelength 1.5418 Å), and X-ray photoelectron spectroscopy (VG ESCALAB MKII spectrometer, Mg KR X-ray source, 1253.6 eV, 120 W) analyses. The specific surface area and gas adsorption isotherms of the adsorbent was tested on a Coulter Omnisorp 100CX Brunauer–Emmett–Teller (BET) using nitrogen adsorption with a degassing temperature of 80 °C.

Adsorption experiments

The As(v) and Cr(vi) stock solutions were prepared with deionized water using $Na_3AsO_4{\cdot}12H_2O$ and K_2CrO_4, respectively. The pH value of the As(v) solution was not adjusted. The pH value of the Cr(vi) stock solutions were adjusted to 6.5 by the addition of HNO_3. The toxic ion working solutions were freshly prepared by diluting the stock solutions with deionized water. The concentrations of the toxic ion species were given as elemental concentrations in this study.

Batch adsorption experiments were conducted to examine the adsorption isotherms of the toxic ions. The adsorption experiments were carried out in 15 mL polypropylene flasks containing 10 mL of the arsenate solution and 0.01 g of the adsorbent. The flasks were then shaken at 150 r min^{-1} in a shaker at 25 °C for 24 h. After the adsorption experiments, the adsorbent was separated from the solution by centrifugation and the residual toxic ion concentration in solution was determined using an inductively coupled plasma atomic emission spectrometer (Jarrell-Ash model ICAP 9000). In the kinetics study, the initial As(v) and Cr(vi) concentrations were 5.20 mg L^{-1}. The adsorbent dose was 1.0 g L^{-1} in the kinetics study. The suspension was placed into an air incubator at an agitation speed of 150 r min^{-1} at 25 °C. About 6 mL suspension was sampled using a pipette at different time intervals. After that the sample was centrifuged and analyzed to determine the concentration of the As(v) and Cr(vi).

Results and discussion

Structures of the γ-FeOOH

Fig. 1a shows the XRD pattern of the obtained product. All diffraction peaks can be indexed to orthorhombic phase γ-FeOOH (JCPDS 44-1415). Fig. 1b presents the XPS Fe 2p spectrum of the as-prepared γ-FeOOH. The binding energies of the Fe $2p_{3/2}$ and Fe $2p_{1/2}$ peaks are located at 710.6 and 724.5 eV, respectively. The Fe $2p_{3/2}$ peak has an associated satellite peak, which is located approximately 8.4 eV higher than the main Fe $2p_{3/2}$ peak. Another satellite peak at 732.8 eV is the satellite peak of Fe $2p_{1/2}$. The satellite peaks result from the charge transfer screening, which can be solely attributed to the presence of the Fe^{3+} ions of γ-FeOOH.[31,32]

Fig. 2a and b present the typical SEM images of the obtained γ-FeOOH. Large amounts of flake-like products were obtained,

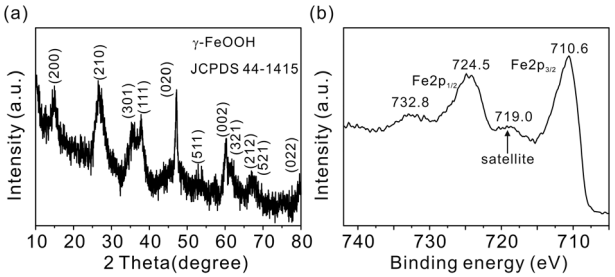

Fig. 1 XRD pattern (a) and XPS Fe 2p spectrum (b) of the obtained γ-FeOOH.

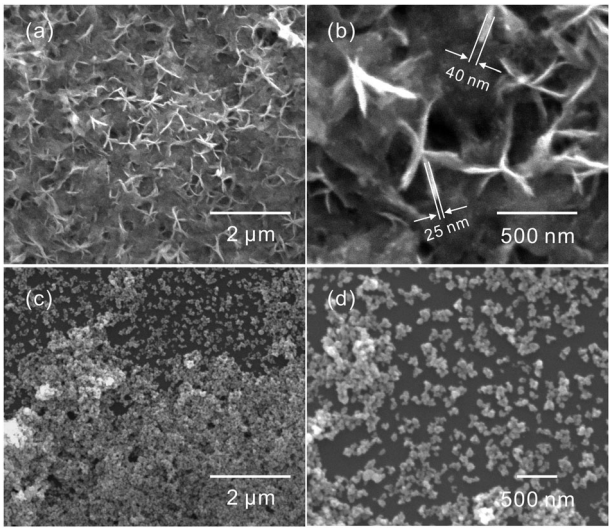

Fig. 2 Low-magnification (a) and high-magnification (b) SEM images of the obtained γ-FeOOH synthesized with EG. SEM images (c, d) of the products synthesized in pure water.

as shown in Fig. 2a. Furthermore, the thickness of these nanoflakes was less than 50 nm, as shown in Fig. 2b. The nanoflakes were assembled together to form 3D structures. In the present work, γ-FeOOH nanoflakes were prepared in a mixture of EG and water. To reveal the role of EG, a control experiment was performed. Fig. 2c and d presents the SEM images of products synthesized in pure water. Only small nanoparticles were obtained. Furthermore, the XRD pattern shown in Fig. 3 suggests that the nanoparticles synthesized in

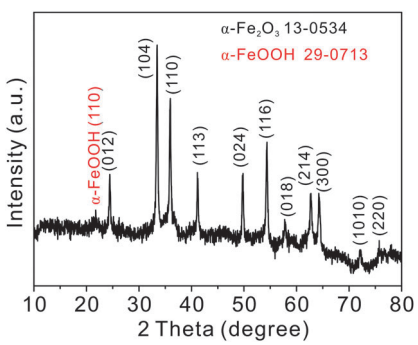

Fig. 3 XRD pattern of the product synthesized in pure water.

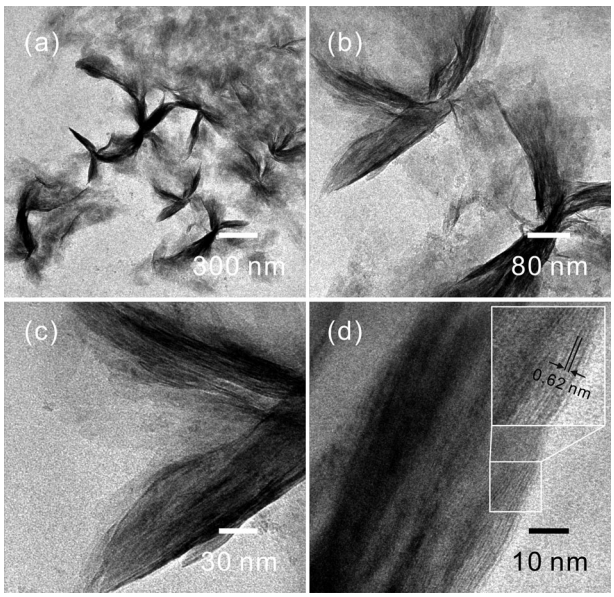

Fig. 4 Low-magnification (a, b) and high-magnification (c, d) TEM images of the obtained γ-FeOOH.

pure water were a mixture of α-Fe_2O_3 and α-FeOOH. It is well known that γ-FeOOH is thermodynamically metastable with respect to α-FeOOH.[13,14] So, the formed α-FeOOH should be the phase transformation product of γ-FeOOH. The generated α-Fe_2O_3 results from the decomposition of α-FeOOH.[14] The results suggest that the presence of EG successfully prevents the phase transformation of γ-FeOOH.

The obtained γ-FeOOH 3D nanoflakes were further characterized by TEM, and the results are shown in Fig. 4. The framework nanostructures were further confirmed by Fig. 4a and b. In addition, the nanoflakes were composed of several thin nanosheets. These nanosheets were assembled together to form a parallel structure, as shown in Fig. 4c. A lattice fringe, with an interplanar spacing of 0.62 nm, was observed, corresponding to the spacing of the (200) planes of γ-FeOOH, as shown in Fig. 4d.

Fig. 5 shows the N_2 adsorption–desorption isotherm and BJH adsorption pore size distribution of the obtained γ-FeOOH products. The isotherm shown in Fig. 5a is type IV with a H1 hysteresis loop, which is characteristic for mesoporous materials.[33,34] The steepness of the capillary condensation step indicates the presence of mesopores, which is further confirmed by the pore size distribution, as shown in Fig. 5b. The BET surface area and the pore volume of the as-prepared γ-FeOOH were 132.8 $m^2\ g^{-1}$ and 0.41 $cm^3\ g^{-1}$, respectively, which were much higher than that of the reported γ-FeOOH.[13,20,35]

As(v) and Cr(vi) removal properties

Metal oxide adsorbents have been widely reported for toxic ion removal from water. Herein, the adsorption properties of the obtained γ-FeOOH 3D nanoflakes towards As(v) and Cr(vi) were investigated at room temperature. The adsorption isotherms are shown in Fig. 6. The obtained adsorption data were well fitted with the Langmuir adsorption model, which was used to represent the relationship between the amount of toxic ions adsorbed at equilibrium (q_e, mg g^{-1}) and the equilibrium solute concentration (C_e, mg L^{-1}).[30,36] The mathematical expression of the Langmuir isotherm is

$$\frac{C_e}{q_e} = \frac{1}{q_m K_L} + \frac{C_e}{q_m}$$

where q_m (mg g^{-1}) is the maximum adsorption capacity and K_L (L mg^{-1}) is the empirical constant. The results suggest that the experimental data could be well fitted with the Langmuir adsorption model with a correlation coefficient value of 0.998 and 0.997, respectively. The Langmuir maximum adsorption capacities of As(v) and Cr(vi) were 45.5 and 17.5 mg g^{-1}, respectively. The maximum adsorption capacity of As(v) was higher than that of Al_2O_3,[4] iron oxides,[5,37,38] $MgFe_2O_4$,[6] Fe_3O_4/MnO_2,[8] CeO_2,[39] CuO,[40] and Mn_3O_4,[41] and similar to nickel carbonate hydroxide,[28] while it was lower than that of Fe_3O_4/NiO,[7] Mg/Al layered double hydroxide[42,43] and MgO.[30] A comparison of the toxic ions adsorption properties of various iron oxides is summarized in Table 1. Accordingly, these results definitely show that the as-prepared γ-FeOOH achieved good adsorption properties.

The kinetics of the adsorption of As(v) and Cr(vi) onto the γ-FeOOH 3D nanoflakes are shown in Fig. 7. The experimental evidence shows that the adsorption rate of As(v) is very fast. Most of As(v) could be removed after one hour. In addition, the adsorption kinetic experimental data can be fitted into a pseudo-second-order rate kinetic model. The pseudo-second-order model is presented as follows[17]

$$\frac{t}{q_t} = \frac{1}{k_2 q_e^2} + \frac{1}{q_e} t$$

where k_2 is the rate constant of the pseudo-second-order model of adsorption, q_t is the amount of As(v) adsorbed on the surface

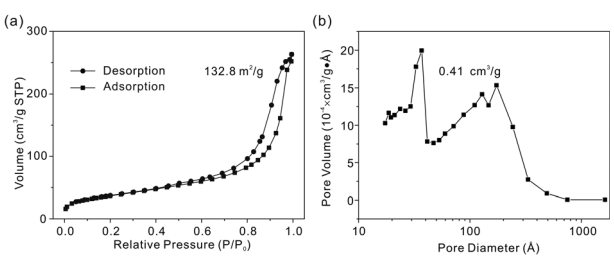

Fig. 5 Nitrogen adsorption–desorption isotherm (a) and the BJH pore-size distribution curve (b) of the obtained γ-FeOOH.

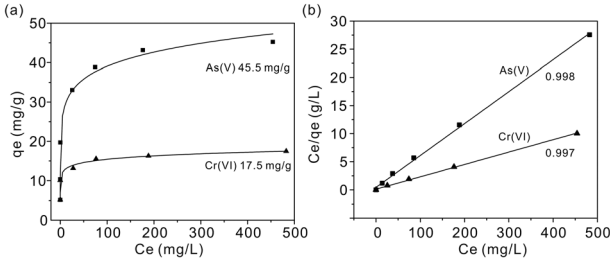

Fig. 6 Adsorption isotherms (a) and linearized Langmuir isotherms (b) obtained from As(v) and Cr(vi) adsorption on γ-FeOOH.

Table 1 Comparison of the toxic ion adsorption properties of various iron oxides

Adsorbents	S (m^2 g^{-1})	As(v) (mg g^{-1})	Cr(vi) (mg g^{-1})	Ref.
Fe_3O_4	34	4.65	4.38	37
α-Fe_2O_3	40	5.31	4.47	37
Fe_3O_4	102	44.1	—	39
α-FeOOH	103	4.7	—	44
α-FeOOH	121	66.2		36
Fe_3O_4/α-FeOOH	41.3	30.2	26.5	10
γ-FeOOH	103.9	32	—	21
γ-FeOOH	132.8	45.5	17.5	This work

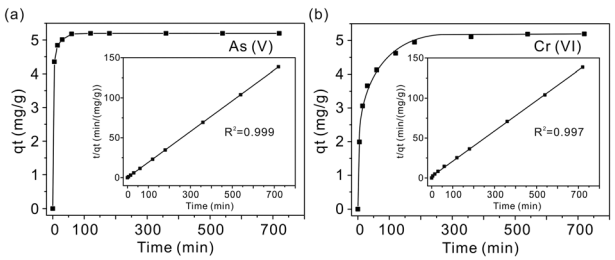

Fig. 7 Effects of contact time on the adsorption of As(v) (a) and Cr(vi) (b) onto γ-FeOOH. The insets present the pseudo-second-order kinetic plots for the adsorption of As(v) and Cr(vi).

of the adsorbent at time t, and q_e is the equilibrium adsorption capacity. For the pseudo-second-order model, the values of k_2 and q_e can be obtained by a plot of t/q_t against t. The pseudo-second-order kinetics plot for the adsorption of As(v) is also shown in Fig. 7. The results suggest that the experimental data could be well fitted with the linear form of the pseudo-second-order model with a correlation coefficient value of 0.999, suggesting that the pseudo-second-order model represents the adsorption kinetics in the adsorbent systems. For Cr(vi) adsorption, the pseudo-second-order model also represents the adsorption kinetics. However, the adsorption rate was much lower than that of As(v), as shown in Fig. 7b. In addition, the γ-FeOOH adsorbent after adsorption was also characterized by XPS. Fig. 8 shows the As 3d and Cr 2p spectra of the adsorbent after adsorption. The results also confirmed the presence of the adsorbed toxic ions.

Previous reports have demonstrated that the surface hydroxyl groups of the adsorbent play a key role in the removal anions.[2,4,10] To reveal the removal mechanism of the γ-FeOOH nanoflakes towards anions, in the process of the kinetics

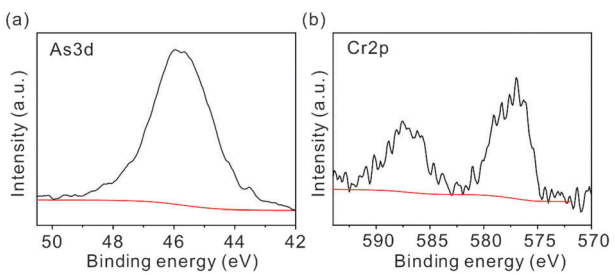

Fig. 8 XPS As 3d (a) and Cr 2p (b) spectra of the adsorbent after toxic ion adsorption.

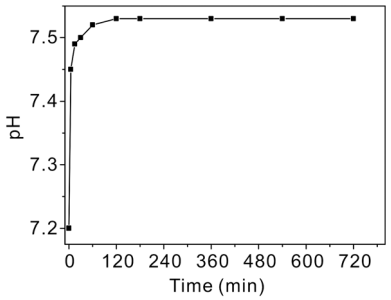

Fig. 9 Effects of contact time on the pH value of the solution.

experiment, the influence of the contact time on the pH value was also investigated, and the results are shown in Fig. 9. The initial concentration of the As(v) ions was 5.20 mg L^{-1}, and the pH value of the solution was 7.20. As can be seen in Fig. 9, the pH value increased rapidly during the first hour, and then gradually reaches a plateau. After 12 hours, the pH value was 7.53. The observed change in pH value was consistent with the adsorption kinetics experimental data, which means that there was an ion-exchange process between the surface hydroxyl groups and the As(v) ions.[4,28]

Effect of coexisting anions on As(v) adsorption

It is well known that some coexisting anions such as Cl^-, SO_4^{2-}, NO_3^-, HCO_3^-, CO_3^{2-}, and PO_4^{3-} are generally present in groundwater, and could interfere in the adsorption process.[38,44,45] To investigate the effect of the above coexisting ions on As(v) removal, these anions were added at three concentration levels (0.1, 1.0 and 10 mM) to the As(v) solutions, and the As(v) removal rate was investigated. Fig. 10 presents the effects of the competing anions on the adsorption of As(v). The experimental evidence suggests that Cl^-, SO_4^{2-} and NO_3^- have no influence on As(v) adsorption. For HCO_3^-, with a concentration lower than 1 mM, the removal rate of As(v) was only slightly decreased. When the concentration of HCO_3^- was increased to 10 mM, the removal rate of As(v) decreased to 90%. The influence of CO_3^{2-} on As(v) adsorption was greater than the ones of HCO_3^-. However, the presence of PO_4^{3-} has a great influence on the removal of As(v). The removal rate markedly decreased to about 30% when the concentration of PO_4^{3-} was

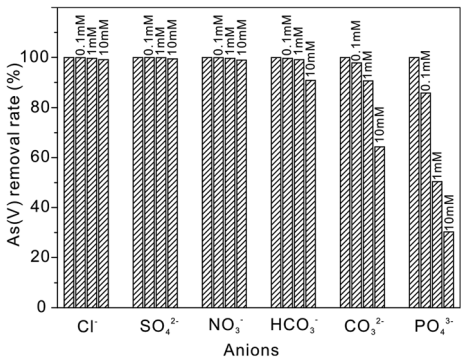

Fig. 10 Effects of competing anions on the adsorption of As(v) (initial concentration 9.97 mg L^{-1}) onto γ-FeOOH.

increased to 10 mM. So, owing to its similar structure to As(v) ions,[44] PO_4^{3-} caused the greatest percentage decrease in As(v) removal at each concentration level, which was consistent with the previous reports.[38,44,45]

Conclusions

A simple EG mediated solution method was demonstrated for the synthesis of γ-FeOOH nanoflakes with a high surface area of 132.8 $m^2\ g^{-1}$. The presence of EG can avoid the phase transformation of γ-FeOOH to α-FeOOH. The removal properties of the obtained γ-FeOOH nanoflakes towards toxic As(v) and Cr(vi) ions were investigated *via* a batch experiment. The adsorption capacities for As(v) and Cr(vi) ions were 45.5 and 17.5 mg g^{-1}, respectively. The equilibrium adsorption data could be well described by the pseudo-second-order kinetic model and the Langmuir equation. The removal of As(v) ions was attributed to ion-exchange, based on the surface hydroxyl groups. The present work provides a new route to fabricate γ-FeOOH nanoflakes with good adsorption properties towards toxic anions.

Acknowledgements

This work was supported by the Natural Science Foundation of Education Committee of Anhui Province (KJ2012A179), the National Key Scientific Program, Nanoscience and Nanotechnology (2011CB933700), the China Postdoctoral Science Foundation (2011M501073), the Natural Science Foundation of Anhui University of Traditional Chinese Medicine (2011zr017B), and the National Natural Science Foundation of China (21103198, 21073197, 11205204 and 61273066).

References

1 E. A. Maull, H. Ahsan, J. Edwards, M. P. Longnecker, A. Navas-Acien, J. B. Pi, E. K. Silbergeld, M. Styblo, C. H. Tseng, K. A. Thayer and D. Loomis, *Environ. Health Perspect.*, 2012, **120**, 1658–1670.
2 W. Z. Sun, Q. Li, S. A. Gao and J. K. Shang, *Chem. Eng. J.*, 2012, **185–186**, 127–135.
3 K. J. Reddy, K. J. McDonald and H. King, *J. Colloid Interface Sci.*, 2013, **397**, 96–102.
4 C. Y. Han, H. P. Pu, H. Y. Li, L. Deng, S. Huang, S. F. He and Y. M. Luo, *J. Hazard. Mater.*, 2013, **254–255**, 301–309.
5 S. Luther, N. Borgfeld, J. Kim and J. G. Parsons, *Microchem. J.*, 2012, **101**, 30–36.
6 W. S. Tang, Y. Su, Q. Li, S. A. Gao and J. K. Shang, *J. Mater. Chem. A*, 2013, **1**, 830–836.
7 S. W. Zhang, J. X. Li, T. Wen, J. Z. Xu and X. K. Wang, *RSC Adv.*, 2013, **3**, 2754–2764.
8 Z. W. Zhao, J. Liu, F. Y. Cui, H. Feng and L. L. Zhang, *J. Mater. Chem.*, 2012, **22**, 9052–9057.
9 K. Amstaetter, T. Borch, P. Larese-Casanova and A. Kappler, *Environ. Sci. Technol.*, 2010, **44**, 102–108.
10 Y. Jia, X. Y. Yu, T. Luo, M. Y. Zhang, J. H. Liu and X. J. Huang, *Dalton Trans.*, 2013, **42**, 1921–1928.
11 M. Lu, A. N. Nikoloski, P. Singh, D. Parsonage, R. P. Das, L. Zhang, W. Li and J. Peng, *Adv. Mater. Res.*, 2013, **634–638**, 249–253.
12 B. Wang, H. B. Wu, L. Yu, R. Xu, T. T. Lim and X. W. Lou, *Adv. Mater.*, 2012, **24**, 1111–1116.
13 J. Majzlan, L. Mazeina and A. Navrotsky, *Geochim. Cosmochim. Acta*, 2007, **71**, 615–623.
14 R. F. Chen, H. X. Chen, Y. Wei and D. L. Hou, *J. Phys. Chem. C*, 2007, **111**, 16453–16459.
15 Z. Shi, J. M. Zachara, L. Shi, Z. M. Wang, D. A. Moore, D. W. Kennedy and J. K. Fredrickson, *Environ. Sci. Technol.*, 2012, **46**, 11644–11652.
16 S. O. Pehkonen, R. Slefert, Y. Erel, S. Webb and M. R. Hoffmann, *Environ. Sci. Technol.*, 1993, **27**, 2056–2062.
17 Y. L. Lin, Y. Wei and Y. H. Sun, *J. Mol. Catal. A: Chem.*, 2012, **353–354**, 67–73.
18 P. Borer, B. Sulzberger, S. J. Hug, S. M. Kraemer and R. Kretzschmar, *Environ. Sci. Technol.*, 2009, **43**, 1871–1876.
19 P. Borer, S. J. Hug, B. Sulzberger, S. M. Kraemer and R. Kretzschmar, *J. Phys. Chem. C*, 2007, **111**, 10560–10569.
20 S. Das, M. J. Hendry and J. Essilfie-Dughan, *Appl. Geochem.*, 2013, **28**, 185–193.
21 E. Repo, M. Mäinen, S. Rengaraj, G. Natarajan, A. Bhatnagar and M. Sillanpää, *Chem. Eng. J.*, 2012, **180**, 159–169.
22 E. E. Carpenter, V. Cestone, G. Landry and V. G. Harris, *Chem. Mater.*, 2003, **15**, 1235–1236.
23 T. Ishikawa, H. Nishimori, I. Abe and K. Kandori, *Colloids Surf., A*, 1993, **71**, 141–146.
24 T. Ishikawa, K. Takeuchi, K. Kandori and T. Nakayama, *Colloids Surf., A*, 2005, **266**, 155–159.
25 A. Jagminas, K. Mažeika, E. Juška, J. Reklaitis and D. Baltrūnas, *Appl. Surf. Sci.*, 2010, **256**, 3993–3996.
26 H. Antony, S. Peulon, L. Legrand and A. Chausse, *Electrochim. Acta*, 2004, **50**, 1015–1021.
27 C. Peng, B. W. Jiang, Q. Liu, Z. Guo, Z. J. Xu, Q. Huang, H. J. Xu, R. Z. Tai and C. H. Fan, *Energy Environ. Sci.*, 2011, **4**, 2035–2040.
28 Y. Jia, T. Luo, X. Y. Yu, J. H. Liu and X. J. Huang, *New J. Chem.*, 2013, **37**, 534–539.
29 Y. Jia, X. Y. Yu, T. Luo, J. H. Liu and X. J. Huang, *RSC Adv.*, 2012, **2**, 10251–10254.
30 Y. Jia, T. Luo, X. Y. Yu, B. Sun, J. H. Liu and X. J. Huang, *RSC Adv.*, 2013, **3**, 5430–5437.
31 T. Yamashita and P. Hayes, *Appl. Surf. Sci.*, 2008, **254**, 2441–2449.
32 L. L. Li, Y. Chu, Y. Liu and L. L. Dong, *J. Phys. Chem. C*, 2007, **111**, 2123–2127.
33 M. Kruk and M. Jaroniec, *Chem. Mater.*, 2001, **13**, 3169–3183.
34 Y. Jia, X. Y. Yu, T. Luo, M. Y. Zhang, J. H. Liu and X. J. Huang, *CrystEngComm*, 2013, **15**, 3647–3653.
35 G. Navarro, R. Acevedo, A. Soto and M. Herane, *J. Phys.: Conf. Ser.*, 2008, **134**, 012023.
36 H. Li, W. Li, Y. J. Zhang, T. S. Wang, B. Wang, W. Xu, L. Jiang, W. G. Song, C. Y. Shu and C. R. Wang, *J. Mater. Chem.*, 2011, **21**, 7878–7881.
37 L. S. Zhong, J. S. Hu, H. P. Liang, A. M. Cao, W. G. Song and L. J. Wan, *Adv. Mater.*, 2006, **18**, 2426–2431.

38 S. X. Zhang, H. Y. Niu, Y. Q. Cai, X. L. Zhao and Y. L. Shi, *Chem. Eng. J.*, 2010, **158**, 599–607.
39 L. S. Zhong, J. S. Hu, A. M. Cao, Q. Liu, W. G. Song and L. J. Wan, *Chem. Mater.*, 2007, **19**, 1648–1655.
40 C. A. Martinson and K. J. Reddy, *J. Colloid Interface Sci.*, 2009, **336**, 406–411.
41 J. G. Parsons, M. L. Lopez, J. R. Peralta-Videa and J. L. Gardea-Torresdey, *Microchem. J.*, 2009, **91**, 100–106.
42 K. H. Goh, T. T. Lim and Z. L. Dong, *Environ. Sci. Technol.*, 2009, **43**, 2537–2543.
43 P. Lakshmipathiraj, B. R. V. Narasimhan, S. Prabhakar and G. B. Raju, *J. Hazard. Mater.*, 2006, **136**, 281–287.
44 G. S. Zhang, H. J. Liu, R. P. Liu and J. H. Qu, *J. Hazard. Mater.*, 2009, **168**, 820–825.
45 G. S. Zhang, J. H. Qu, H. J. Liu, R. P. Liu and R. C. Wu, *Water Res.*, 2007, **41**, 1921–1928.

